Journal of Dentistry 116 (2022) 103902

Contents lists available at ScienceDirect

Journal of Dentistry

journal homepage: www.elsevier.com/locate/jdent

Fracture resistance of cantilevered full-arch implant-supported hybrid prostheses with carbon fiber frameworks after thermal cycling

Evelina Haroyan-Darbinyan [a], Marta Romeo-Rubio [a], Jaime Del Río-Highsmith [a,*], Christopher D. Lynch [b], Raquel Castillo-Oyagüe [a,*]

[a] Faculty of Dentistry, Complutense University of Madrid (U.C.M.), Madrid, Spain
[b] University Dental School & Hospital/University College Cork, Wilton, Cork, Ireland

ARTICLE INFO

Keywords:
Full-arch implant-supported hybrid prostheses
Cantilever
Prosthetic frameworks
Carbon fiber
Cobalt-chromium
Resin veneering

ABSTRACT

Objectives: This in vitro study aimed to find the best combination of mesostructure and veneering materials for full-arch implant-supported hybrid prostheses (HPs) in terms of the fracture resistance (FR) of their cantilevers.
Methods: Three groups ($n = 5$ each) of maxillary HPs were fabricated: Group-1 (CC-A, *control*): Co-Cr frameworks coated with acrylic resin; Group-2 (CF-A): carbon fiber veneered with acrylic resin; and Group-3 (CF-R): carbon fiber coated with composite resin. All specimens were submitted to 5,000 thermal cycles (5 °C – 55 °C, dwell time: 30 s), and subjected to a single cantilever bending test in a universal testing machine (crosshead speed: 0.5 mm/min) until failure. The fracture pattern was assessed using stereo microscope and SEM. The one-way ANOVA and Bonferroni tests were run ($\alpha = 0.05$).
Results: The FR yielded significant differences among the three groups ($p < 0.001$). CC-A samples reached the highest FR values ($p \leq 0.001$), whereas both CF-A and CF-R HPs exhibited the comparably ($p = 0.107$) lowest FR. CC-A specimens failed cohesively (100%): mostly without chipping (80%). CF-A mesostructures were always broken at the connections of the distal implants. CF-R prostheses often failed adhesively (80%).
Conclusions: The HPs made of Co-Cr veneered with acrylic demonstrated the best mechanical behavior, being the only group whose 13-mm long cantilevers exceeded the clinically acceptable FR of 900 N. The HPs constructed with carbon fiber frameworks showed, additionally, more unfavorable fracture patterns.
Clinical significance: For HPs with cantilevers up to 13 mm, Co-Cr mesostructures coated with acrylic may represent the optimum combination of materials.

1. Introduction

Cantilevered full-arch implant-supported hybrid prostheses (HPs) have become an alternative prosthodontic treatment with high survival rates in the challenging situations of edentulous patients with augmented prosthetic spaces, intense alveolar bone loss, and lack of adequate support for the soft tissues [1–3]. According to the Bränemark original protocol, these screwed restorations with distal cantilevers in both hemiarcades [4] were first fabricated with cast gold frameworks coated with acrylic resin, in which acrylic denture teeth were embedded [4,5]. However, given the price of this noble metal, different alloys such as those based on silver-palladium [6], titanium [7], or cobalt-chromium have been used instead [8].

Notwithstanding the popularity of HPs, several studies highlight their prevalence of complications, which often result in multiple maintenance and repair appointments to keep them functional [9–12]. The presence and length of the cantilevers [13], the lack of fine proprioception [14], the type of antagonist [15], the parafunctional overloading [16], and the poor union of the coating material to the metallic framework [17,18], are the main risk factors associated to the failure of these fixed implant rehabilitations. Even though the retention between acrylic resin and metal alloys has been tried to be improved [19–21], the detachment and/or fracture of the artificial teeth and of the prosthetic gingival tissues are still the most common failure-causing problems in HPs, alongside the wear of the occlusal surfaces [11,12].

On the one hand, the absence of a chemical adhesion between the

* Corresponding authors at: Department of Conservative & Prosthetic Dentistry, Faculty of Dentistry, Complutense University of Madrid (U.C.M.), Pza. Ramón y Cajal s/n, 28040 Madrid, Spain.
E-mail addresses: evelinah@ucm.es (E. Haroyan-Darbinyan), mromeo@pdi.ucm.es (M. Romeo-Rubio), jrh@ucm.es (J.D. Río-Highsmith), chris.lynch@ucc.ie (C.D. Lynch), raquel.castillo@ucm.es (R. Castillo-Oyagüe).

https://doi.org/10.1016/j.jdent.2021.103902
Received 10 October 2021; Received in revised form 15 November 2021; Accepted 17 November 2021
Available online 22 November 2021

acrylic components and the metallic mesostructure may result in microleakage at the junction, fluid percolations, microgaps, and deterioration of the acrylic resin [22]. On the other hand, the differences in the coefficients of thermal expansion (CTEs) between the acrylic suprastructure and the metallic framework in combination with the volumetric shrinkage of the acrylic resin, have also been related to the bond failure at the acrylic/metal interface [23,24]. In recent years, the need of overcoming these drawbacks has led to the development of metal-free materials such as carbon fibers, which seem to provide similar stiffness [25–29]. Nonetheless, very few studies address the mechanical properties of these new mesostructures when bonded to acrylic or composite resin [25,26,29]. Furthermore, there are no investigations focusing on the fracture resistance of the distal cantilevers of HPs made with such combinations of materials, despite the fact that the cantilever is the most fragile area. In this respect, maxillary cantilevers ranging between 10 and 12 mm [30] and between 12 and 15 mm [31,32] have been recommended. However, most authors agree that the extensions should be as short as possible, in order to avoid biomechanical problems [33]. We have selected 13-mm long cantilevers for being loaded in our experiment, as this value is the promedium of those suggested in the literature, and because this measure covers the mesio-distal dimension of two premolars for a shortened dental arch (SDA).

Therefore, this investigation aimed to find the best combination of framework and veneering materials for HPs in terms of the fracture resistance (FR) of their cantilevers, and to determine whether the FR values obtained in the study groups exceeded the clinically acceptable limit of 900 N (taken as an empirical reference) [34]. Thus, the null hypothesis tested was that maxillary HPs made of acrylic coated cobalt-chromium (CC-A), carbon fiber veneered with acrylic resin (CF-A), and carbon fiber covered with composite resin (CF-R) show no significant differences to each other concerning the FR and fracture pattern of their cantilevers.

2. Material and methods

2.1. Sample size calculation

The FR mean and standard deviation (SD) values registered from five specimens per group were used to calculate the sample size (Nquery Sample Size Software® v. 7.0, Statsols®, Boston, MA, US). A power of 95% and a significance level of α= 0.05 were considered [35]. A minimum of three specimens per group was estimated to obtain reliable findings. Therefore, the five specimens tested in each experimental group were maintained to achieve a larger effective sample size [25,36,37]. The pilot study was thus validated as the definitive investigation.

2.2. Specimens' design and manufacturing procedures

For our in vitro study, 15 maxillary full-arch hybrid implant-supported prostheses (HPs) were CAD/CAM fabricated. Depending on their framework (mesostructure) and veneering (suprastructure) materials, together with their associated manufacturing procedures, these rehabilitations were assigned to the following groups (n = 5 each). Group 1 (CC-A, *control*): Acrylic-coated cobalt-chromium HPs; Group 2 (CF-A): Acrylic-coated carbon fiber HPs; and Group 3 (CF-R): composite-resin veneered carbon fiber HPs.

All of the samples were manufactured by the same prosthodontic technician, who used a stainless-steel machined support that contained five cylindrical dental implants with an external hexagonal connection, a 3.75 mm wide platform, a length of 10 mm, and a diameter (Ø) of 4.1 mm (Nobel Biocare®, Gothenburg, Sweden). These fixations were inserted in the 14, 12, 11, 22, and 24 arch positions. The metallic model was digitized (3Shape® D2000 Dental System, Copenhagen, Denmark). A framework for a maxillary full-arch cantilevered HP with a SDA was computer-aided designed (CAD) (Fig. 1A). Such STL archive was sent to a milling device (VHF- S2, VHF, Ammerbach, Germany), in which five equal structures were machined from cobalt-chromium (Co-Cr) disks (imes-icore GmbH®, Eiterfeld, Germany); and ten identical structures were milled from 100% carbon fiber disks (Micromedica®, Robbio, Italy). The last ones were randomly assigned to the Groups 2 and 3 (n = 5 each). After being machined, all of the samples were cleaned with water steam and gently air-dried.

A wax pattern of the suprastructure was manually prepared (Bader®, Nigrán, Pontevedra, Spain) and a silicone mold was obtained from the mock-up (Glass Silicon®, Micromedica®) to ensure that all of the HPs had the same dimensions and morphology.

In the CC-A group *(control)*, the Co-Cr frameworks were impregnated with metal bonding (Link®, Ivoclar-Vivadent®, Schaän, Liechtenstein) and were coated with two layers of wash opaque paste (Opaquer Nexco®, Gingiva Opaquer®, Ivoclar-Vivadent®) that masked the underling metallic color. The carbon fiber frameworks of the CF-A and the CF-R groups were varnished with a compatible adhesive (BioxFill®, Micromedica®) and their darkness was then neutralized with two layers of special wash opaque material (BioxFill® Opaquer Medium, Micromedica®). All of the structures were light-cured for 3 min both after the adhesive and the opaque application using the same curing unit (HiLite® Power, Heraeus, Hanau, Germany).

In the acrylic-veneered groups (CC-A and CF-A), the wax pattern facilitated the precise placement of the denture teeth and the direct conformation of the soft tissues. For the construction of each HP, the artificial teeth (SR Orthotyp®, Ivoclar-Vivadent®) were fitted in their respective positions into the silicone mold. Immediately after, heat-curing acrylic resin (Paladon 65 Pink®, Kulzer®, Tokyo, Japan) was

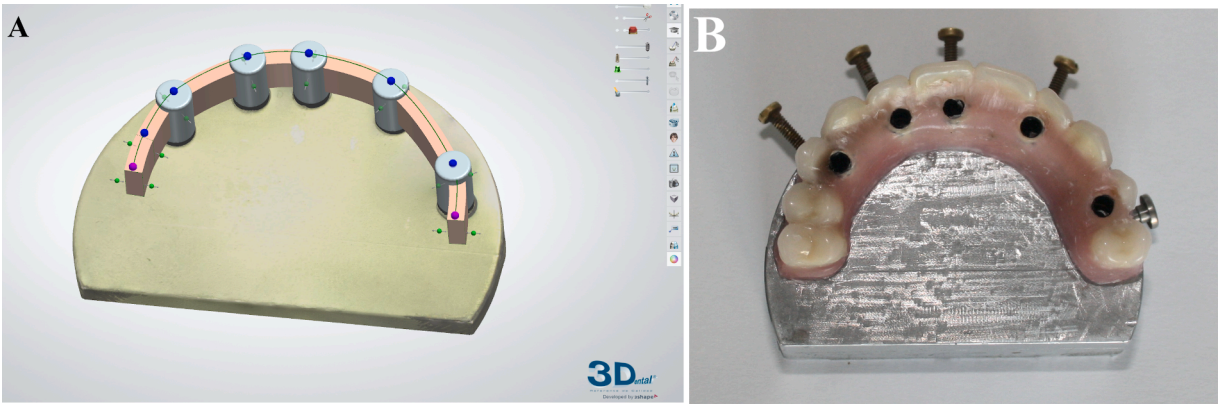

Fig. 1. A: Digital design of the framework of all the implant-supported hybrid restorations. **B:** Study sample that mimicked a real maxillary hybrid prosthesis, composed, in this case, by a carbon fiber mesostructure coated with acrylic resin (Group 2).

poured in the muffle with the framework and was processed in a curing machine (Mestra 030,420®, Mestraitua S.L., Bilbao, Spain) for 15 min, at 55 °C (131°F), and 2 bars of pressure. The acrylic excesses and irregularities were trimmed using conventional handpiece burs. All of the specimens were polished using an electropolishing device with a cotton brush (Mestra®). In the CF-R group, the artificial teeth and the prosthetic gum were made-up with composite resin (Nexco® A2, Ivoclar-Vivadent®) using the layering technique inside the silicone mold. In this group, each 2-mm film of composite resin was light-polymerized in the curing unit (Hilite® Power).

Finally, the connections at the mesostructure/implant interfaces were sandblasted with 100 μm Ø aluminum oxide (Al_2O_3) particles (distance: 5 cm, pressure: 1 kg), and were steam cleaned. The connections of the CC-A prostheses were then treated with metal adhesive primer (Monobond Plus®, Ivoclar-Vivadent®) and were luted to the mesostructure using a self-healing agent (Multilink Hybrid Abutment®, Ivoclar-Vivadent®). The connections of the CF-A and CF-R groups were bonded to the carbon fiber frameworks with an appropriate cement (Carboblock®, Micromedica®).

2.3. Artificial aging

In the chemical laboratory of our Faculty, 10 L of artificial saliva (pH= 7) were produced with this formulation (in g/L): NaCl (0.4); KCl (0.4); $CaCl_22H_2O$ (0.906); $NaH_2PO_42H_2O$ (0.0690); Na_2S9H_2O (0.005); and urea (1). The aging protocol for biomaterials outlined in the ISO/TR 11,405:2015 standard was strictly followed. The specimens were thermal cycled for 5000 cycles in the artificial saliva (dwell time: 30 s, transfer time between consecutive cycles: 2 s) in a custom-made thermal cycling machine, with temperatures ranging from 5 °C (41°F) to 55 °C (131°F). This aging procedure would correspond to 1 year of clinical service [38].

2.4. Single cantilever bending test

After aging, the samples were kept stored in artificial saliva at 37 °C (98.6°F). Immediately before the bending test, the specimens were dried with an absorbent cloth and were labeled with an alphabetical code that corresponded to the group acronyms. Within each group, the restorations were randomly differentiated by subscript numbers from 1 to 5.

All of the specimens (Fig. 1B) were subjected to a flexural load through a single cantilever bending test in a universal testing machine (UTM). This electromechanical tool (MTS Insight 45®, Eden Prairie, US) has a maximum capacity of 100 kN, an accuracy of ± 0.5% of the force exerted, and a speed precision of ± 0.1% of the chosen speed. The UTM was calibrated by an engineer according to the ISO 7500 and ASTM E4 standards, one month before our investigation. The standard error of measurement of the bending test was 367,504 (SD of the scale at baseline= 489,35,383; Chronbach's α= 0.4355).

The machined support that contained the implants was horizontally oriented and screwed to the metallic plate of the UTM. Before testing, each restoration was anchored to the implants of the master model. Standard titanium screws (IPD®, Barcelona, Spain) were tightened to 30 Ncm [3] throughout all the cemented connexions of each HP by means of an electronic torque wrench (Nobel Biocare Torque Controller®, Gothenburg, Sweden).

The load was always applied in the right hemiarcade, at the mesiodistal midpoint between the implant in position 14 and the end of the 13 mm-long cantilever. A Ø 10 mm stainless-steel round ended cylindrical punch was fixed to the load cell and was adjusted to the marked location in each sample (6.5 mm distally to the center of the 14 implant connection, coinciding with the vestibular-lingual midpoint). A vertical force with an initial module of 0.2 N was exerted at a crosshead speed of 0.5 mm/min until the fracture and/or the detachment of the veneering material occurred. Thanks to these parameters the failure type was analysed in detail. An evident decrease in the stress plot of the loading curve announced the failure initiation, which was also recognized throughout visible and audible signs of cracks. The data obtained were interpreted using the TestWork® software (MTS®, Eden Prairie, US).

The bending test was entirely performed by a trained, single operator. The same conditions of room temperature (RT: 23.0 ± 1.0 °C, i.e., 73.4 ± 33.8°F) and relative humidity (RH: 50 ± 5%) were maintained [39].

2.5. Classification of the fracture pattern

The failure modes were evaluated by an experienced, single rater, and were classified into different categories: 'adhesive' (debonding of the coating material), 'cohesive' (showing cracks with or without chipping within the thickness of the suprastructure), 'mixed' (almost equilibrated combination of both adhesive and cohesive modalities), and 'complete failure' (a breakage of the mesostructure also occurred).

2.6. Stereoscopic and SEM evaluation

After the bending test, the failure modes were examined under stereo microscope (Leica M80®, Heerbrugg, Switzerland), at 40 × magnifications, with a LED light source (CLS 100 Leica®). Images of the fractured sites were taken using the Leica DFC 450® digital camera (5 megapixel CCD sensor).

Specific fractured areas of the HPs from each group were explored using different magnifications (100 × and 300 ×) under scanning electron microscope (SEM; JSM-6400®, Jeol®, Tokyo, Japan). The SEM images had a tridimensional (x/y/z) resolution of 4 nm at an accelerating voltage of 20 kV [39]. In view of the curvilinear design of the prostheses, the samples were alternatively fitted on their support for getting the best projection angles with respect to the optical axis of the microscope [40].

Before SEM evaluation, the samples' surfaces were sputtered homogeneously with a 10 nm thick gold film in a metallizing machine (Quorum Q150R S®, East Sussex, UK). This device has a vacuum chamber with argon (Ar) gas (in whose rotating base the specimens are placed), and a cover with a pure gold layer that is connected to the electrodes. The procedure begins by emptying the chamber at 3×10^{-2} Mbar, thus generating a potential difference of 20 mA, and continues by removing the Ar from the chamber. This preparation is necessary to avoid distortion in non-conductive specimens before being SEM assessed. A specialized technician metallized the HPs and managed the SEM under our supervision.

2.7. Statistical analysis

The fracture resistance (FR) values were analysed using a specific software (Stata 16.1®, StataCorp®, Texas, US). Descriptive statistics were reported as means with standard deviations (SD), medians, interquartile ranges (IQR), and minimum and maximum values in Newton (N).

As the Shapiro-Wilk test confirmed the normality of the distribution (p> 0.05) [41], parametric probes were selected. The one-way analysis of variance (ANOVA) followed by the *post hoc* Bonferroni pairwise comparison test were run. Saving the methodological disparities, the FR data were processed according to well-established statistical methods used in related research [25,42]. The significance level was set in advance at α= 0.05 [39,40,42]. The frequency of appearance of the categorized failure modes was expressed in percentages within each experimental group (qualitative variable) [43].

3. Results

3.1. Fracture load

All of the samples remained intact after thermal cycling. The FR

statistics are outlined in Table 1. The spread and centers of the set of FR values recorded per group are presented in Fig. 2 with box and whiskers plots.

The tested groups of maxillary HPs yielded statistically significant differences ($p < 0.001$), which were registered between the CC-A and CF-A groups ($p = 0.001$), and between the CC-A and CF-R groups ($p < 0.001$). On the contrary, the CF-A and CF-R groups showed statistically comparable FR values ($p = 0.107$).

Thus, the CC-A samples achieved the significantly highest FR in the study (1364.9 ± 256.2 N), whereas both the CF-A (655.4 ± 262.9 N) and CF-R (331.8 *N* ± 73.1 N) groups evidenced the comparably lowest FR values under our experimental conditions.

Only the CC-A samples exceeded the predetermined clinically acceptable minimum FR of 900 N at the tested location.

3.2. Microscope analysis and fracture pattern

Exemplary images of the tested samples taken by stereo microscope (40 ×) and by SEM (100 × and 300 ×), are displayed in the Figs. 3-5. We started by evaluating the site of initiation and also the propagation of the fracture lines, as well as the superficial cracks by using 40 × magnifications with the stereo microscope. Subsequently, 100 × magnifications were programmed in the SEM to assess the disengaged elements, to explore possible micro-gaps and to examine the different broken parts classifying them through a by-component basis (acrylic resin, composite resin, carbon fiber, cobalt-chromium, cement, etc.). Finally, once the failure type had been identified, 300 × magnifications were used to look for particles and material residuals on the surfaces of each mesostructure and suprastructure [36,39,40].

In the CC-A group, the failure mode was cohesive in all cases, so that the mesostructures preserved their integrity. Even more, 80% of the prostheses in this group presented a superficial crack without chipping of the acrylic coating (Table 2, Fig. 3A). Remnants of the adhesive used for bonding the acrylic to the Co-Cr substrate and/or traces of the opaque paste were frequently discovered by SEM in the CC-A group, which confirmed the cohesive fracture pattern (Fig. 3B).

In the CF-A group, a complete failure or framework fracture was always registered at the interface between the mesostructure and the distal implant connection. Vestiges of bonding/coating materials were commonly identified on the implant surfaces (Table 2, Fig. 4A). At the fracture line, the separation between the carbon fiber framework and the acrylic coating was verified by SEM, and slight fragments of some broken carbon fibers that remained attached to the acrylic material could be seen (Fig. 4B).

As for the CF-R prostheses, the framework of an isolated specimen was completely broken at the access hole of the implant adjacent to the cantilever, showing a preponderant adhesive fracture pattern (Table 2, Fig. 5A). Most samples of this group (80%) failed adhesively without the breakage of the mesostructure, so that the composite resin was disengaged from the carbon fibers. Actually, in this group, residues of the debonded materials were hardly observed on the opposite surfaces (Fig. 5).

Table 1.
Fracture load values (N) of the implant-supported hybrid prostheses after the cantilever bending test.

Group	*n*	Mean	SD	Me	IQR	Min	Max
CC-A	5	1364.9 (a)	256.2	1445.1	399.4	1038.9	1629.2
CF-A	5	655.4 (b)	262.9	590.0	132.1	372.1	1080.0
CF-R	5	331.8 (b)	73.1	334.8	64.7	245.1	438.9

N: Newton. **CC-A (Group 1):** Implant-supported hybrid prostheses (HPs) made of Co-Cr frameworks coated with acrylic resin. **CF-A (Group 2):** HPs with carbon fiber mesostructures veneered with acrylic resin. **CF-R (Group 3):** HPs with carbon fiber frameworks coated with composite resin. **SD:** Standard deviation. **Me:** Median. **IQR:** Interquartile range. **Min:** Lowest fracture resistance (FR) value registered in each group. **Max:** Highest FR value recorded in each group. In the third column, different lowercase letters indicate statistical differences ($p \leq 0.001$).

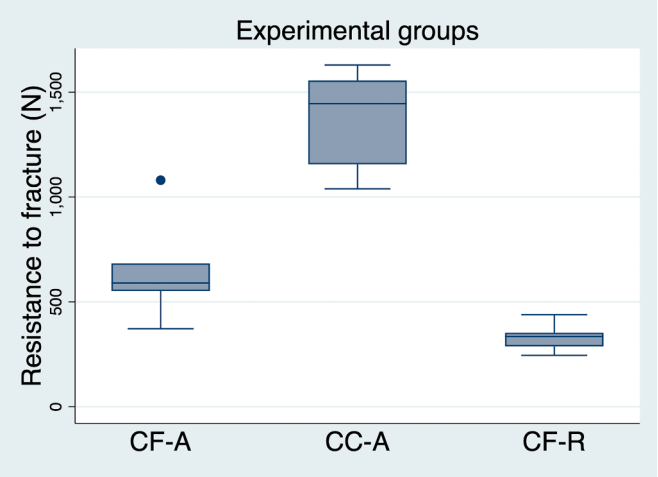

Fig. 2. Box Plot that graphically depicts the spread-out of the fracture load (FR) data recorded in the experimental groups after the single cantilever bending test.

4. Discussion

The mechanization of the HPs' mesostructures from carbon fiber disks is part of the advancement of the CAD/CAM technologies. However, to date, these materials have been scarcely investigated [25–29]. Our null hypothesis was rejected, because the tested groups of HPs showed significantly different FR values and diverse fracture patterns at their cantilevers.

Starting by the analysis of the fracture strength, the CC-A restorations presented the significantly highest FR, which comfortably overtook the 900 N preset for clinical acceptability (Table 1, Fig. 2). Together with food impaction, speech problems, and difficulties to cope with the daily hygiene routines [44,45], the worst disadvantages of acrylic coated Co-Cr HPs have traditionally been biomechanical failures and component fractures by deflection [9–12]. Nevertheless, our CC-A samples exhibited significantly higher FR values than did both the CF-A and CF-R groups, which attained statistically comparable results (Table 1, Fig. 2). In comparison with both types of carbon fiber HPs, the Co-Cr veneered with acrylic resin was the most resistant combination of materials for maxillary HPs at their 13-mm long cantilevers.

The mechanical behavior of the HPs constructed with carbon fiber mesostructures is controversial [25-29,46-52]. A high resistance to flexural loads has been reported for implant-supported fixed dental prostheses made with carbon fiber coated with acrylic [25,26]. Nonetheless, the disparities in the laboratory work techniques; the orientation, cutting mechanisms, pretreatments, structural properties, and composition of the carbon fibers; the loading sites and, overall, the experimental protocols, make the comparisons almost unfeasible [25, 26,46-52]. None of the cited investigations used samples that mimicked real HPs. As no previous studies have compared the FR and fracture pattern of HPs made with carbon fiber and metallic structures after cantilever bending tests, our results cannot be rigorously contrasted.

Menini et al. [25,29] compared carbon fiber-reinforced composite structures and gold alloy frameworks, suggesting that the first ones might be a viable alternative to the traditional metallic structures for fixed implant-supported restorations. It must be highlighted that all of our mesostructures were milled from Co-Cr and pure carbon fiber disks, instead of being: manually layered, reinforced with composite, and adapted to the desired design, as they were in the mentioned research [25,29]. Moreover, in our study, a unique wax pattern was elaborated to keep the same configuration in all samples.

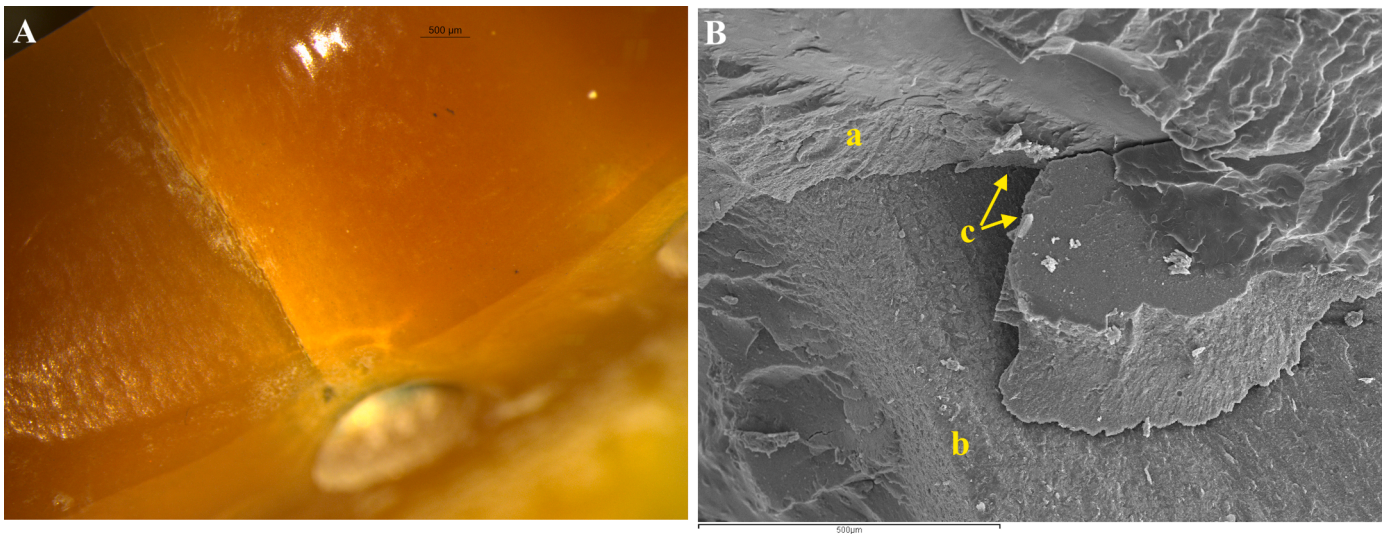

Fig. 3. **A:** Stereoscopic image (40 ×, bar: 500μm) of the CC-A_3 specimen. A little crack without chipping of the acrylic coating may be observed. **B:** SEM micrograph taken at the fractured area of the CC-A_1 sample (100 ×, bar: 500μm). Reduced vestiges of remaining adhesive and opaque paste are obvious. The acrylic resin coating has been marked with the 'a' lowercase letter; 'b' points to the metallic framework, and 'c' shows both a microgap between the mesostructure and the veneering material, and a linear crack on the prosthesis' surface.

Table 2.
Percentages of failure types observed after the cantilever bending test.

Group	*n*	Failure mode (%)	Failure location
CC-A	5	C (20%) Cr (80%)	Acrylic resin coating
CF-A	5	F (100%)	Framework / chimney interface
CF-R	5	F (20%) A (80%)	Framework / chimney interface Composite resin veneering

CC-A (Group 1): Implant-supported hybrid prostheses (HPs) made of Co-Cr frameworks coated with acrylic resin. **CF-A (Group 2):** HPs with carbon fiber mesostructures veneered with acrylic resin. **CF-R (Group 3):** HPs with carbon fiber frameworks coated with composite resin. **C:** Cohesive failure (within the veneering material). **C—Cr:** Subtype of cohesive failure consisting on the appearance of cracks without detachment of the suprastructure material. **A:** Adhesive failure (debonding of the coating material). **F:** Complete failure (which moreover involves framework fracture).

Clinically, Pera et al. [28] observed that full-arch screw-retained immediate prostheses with frameworks made of carbon fiber-reinforced composite registered high survival rates at a mean follow-up period of 22 months. Conversely, a longitudinal multicenter study carried out by Yong and Moy [46] reported unsatisfactory mechanical properties for immediately loaded HPs made of acrylic-coated carbon fibers, as the implants recorded an overall failure rate of 9% and the breakage of the restorations at the distal abutments was the main late prosthetic complication [46]. Our distal implant connections were also critical areas (Figs. 4A and 5A) [42,46]. Concretely, this failure mode was always recorded in our CF-A group (Table 2, Fig. 4), and also detected in one CF-R specimen (Table 2, Fig. 5A). Probably, the lower thickness of the carbon fiber material next to the implant access holes may help explain this fracture pattern.

The masticatory load intensity may rely on diverse factors, but, generally, forces of around 900 N have been measured in posterior

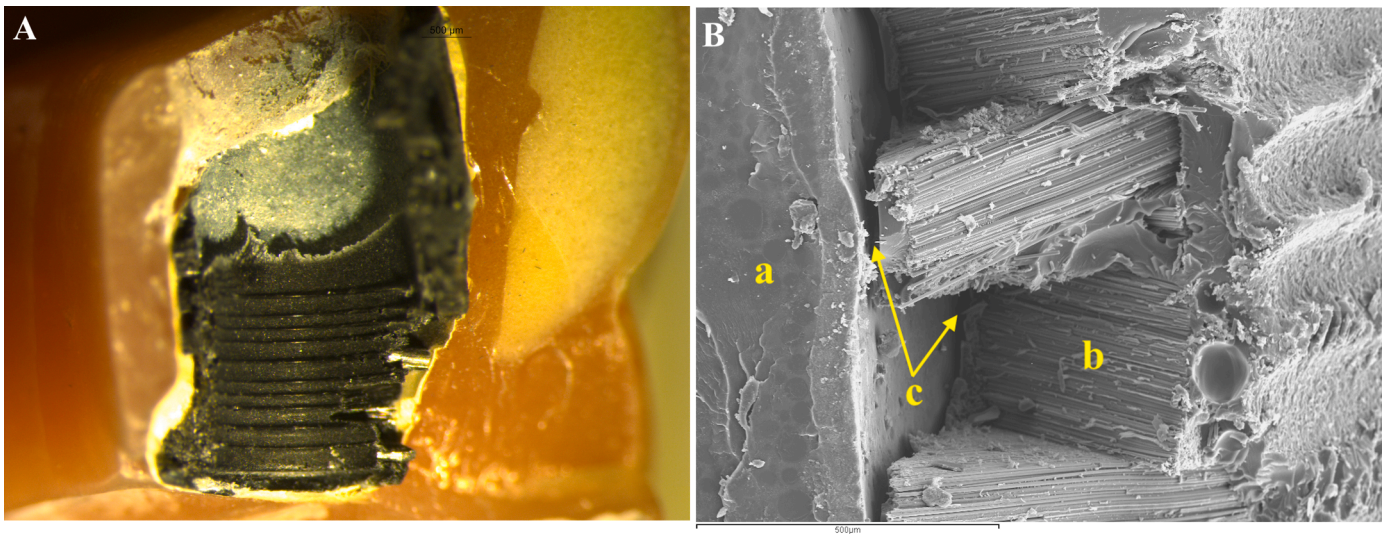

Fig. 4. **A:** Stereoscopic image (40 ×, bar: 500μm) of the CF-A_4 restoration. The specimen was totally fractured at the level of the distal implant. Residuals of bonding/coating materials may be appreciated on the implant surface. **B:** SEM micrograph (300 ×, bar: 500μm) of the CF-A_2 hybrid prosthesis, in which the lowercase letters indicate: the acrylic coating with a regular topography, almost flat ('a'), the cross-linked carbon fibers of the framework ('b'), and a visible disjunction between the veneering material and the mesostructure ('c'). Small traces of carbon fibers adhered to the acrylic resin, are detectable.

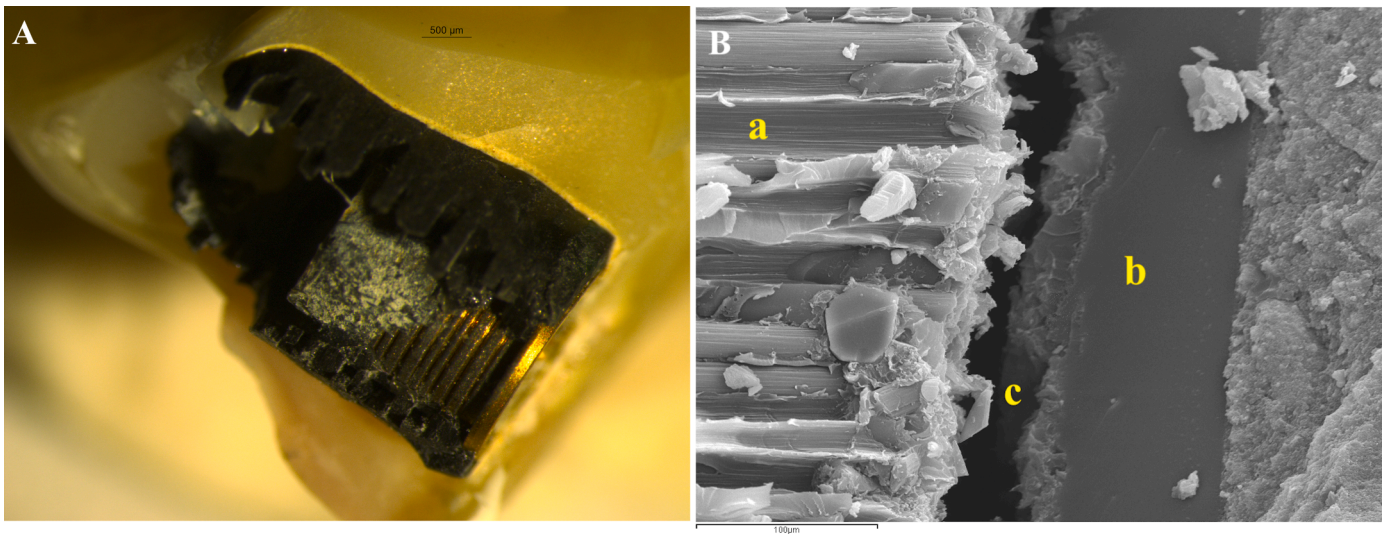

Fig. 5. A: Stereoscopic image (40 ×, bar: 500μm) of the CF-R_4 sample. A complete breakage of the framework with a predominant adhesive fracture pattern is evident at the distal connection site. **B:** SEM micrograph (300 ×, bar: 100 μm) of the CF-R_3 specimen, which presents an adhesive failure with a total separation between the carbon fiber filaments ('a') and the composite resin coating material ('b'). The microgap between the composite veneering and the carbon fiber mesostructure is noticeable ('c').

sectors of adult dentate patients [34]. Given that parafunctional forces can reach 1000 N, some authors argue that dental restorations should ideally withstand this load [53–55]. In our study, only the HPs made of Co-Cr surpassed both values (Table 1, Fig. 2). After implant rehabilitation, the maximal bite force of edentulous patients usually increases [56,57]. Hence, while the HPs made of acrylic coated Co-Cr seem to provide clinically acceptable FR values at the cantilevers (Table 1, Fig. 2), carbon-fiber based HPs might be, at most, considered for anterior areas, with lower maximal bite forces [58].

Taking into account that previous researchers exerted the load between implants or at intermediate positions [25,26] and/or used unrealistic samples [25,28,42], their findings cannot be extrapolated to the cantilevers, which are the most fragile areas. Moreover, the CAD/CAM fabrication of our HPs minimized the handwork, limiting this confounding variable [26,42].

In another vein, the specimens failed with varying degrees of severity and distinct fracture patterns. In the CC-A group, only one specimen showed a slight chipping of the acrylic coating (Table 2), adjacent to the posterior implant connection. The remaining CC-A samples just recorded superficial cracks (Table 2, Fig. 3A). Thus, the FR values together with the characteristical cohesive failure in this group (mainly without chipping) suggest that the union between Co-Cr and acrylic has yet to be overtaken by carbon fiber prostheses, regardless of the veneering material (Tables 1 and 2, Fig. 2). In the CF-A group, all of the HPs were broken at the distal implants (Table 2, Fig. 4A), with visible remnants of the bonding and/or coating materials on their surfaces. A clear disengaging of the coating material with scarce ends of the broken fibers still bonded to the acrylic resin were observed (Fig. 4B). According to Menini et al. [29], in our CF-R group, the predominant failure type was adhesive (Table 2). In this set, the composite resin was debonded from the framework substrate (Fig. 5B). This may be due to the different Young's modulus of both materials, as the composite resin is more rigid than the carbon fiber [59,60]. The complete failure registered in one CF-R specimen left the exposed implant surface practically free of residues, according to the prevalent adhesive failure mode in this group (Fig. 5A). An adhesive failure reveals a weak framework/suprastructure union, which is in accordance with the low FR values achieved by the CF-R samples (Table 1, Fig. 2).

Future research should determine the minimum appropriate thickness for carbon fiber structures, while the bonding and veneering protocols should be enhanced. Even though a single operator performed the experimental work in order to ensure a standardized process [61], our FR data must be cautiously extrapolated to the clinical setting, since the complex biotermal mechanical factors of the oral environment are not considered in vitro tests. Other relevant aspects, such as the quality of life provided by carbon fiber HPs, should be compared with the positive results achieved so far with the traditional HPs made of acrylic-coated Co-Cr [62,63].

5. Conclusion

Within the limitations of our study, these conclusions may be drawn:

1 For full-arch maxillary hybrid implant-supported prostheses (HPs) with cantilevers up to 13 mm, Co-Cr mesostructures coated with acrylic resin may represent the optimal combination of materials in terms of the fracture resistance of their cantilevers.
2 Regardless of their veneering material (acrylic or composite resin), the cantilevers of carbon fiber HPs were significantly less resistant than those of acrylic-coated Co-Cr HPs; this being the only group that exceeded the clinically acceptable limit of 900 N at such location.
3 The HPs made of Co-Cr veneered with acrylic exhibited cohesive failures that mainly consisted of cracks without chipping, which is the least critical fracture pattern. Conversely, a complete breakage of all acrylic-coated carbon fiber HPs occurred next to the distal implants, while most composite-veneered carbon fiber prostheses failed adhesively.
4 Considering the lack of research on the fracture resistance and failure modes of the HPs' cantilevers with carbon fiber mesostructures, more related in vitro and protocolised in vivo studies are required to confirm our findings prior to their clinical extrapolation.

Funding

This research did not receive any specific grant from funding agencies in the public, commercial, or not-for-profit sectors.

CRediT authorship contribution statement

Evelina Haroyan-Darbinyan: Conceptualization, Methodology, Investigation, Data curation, Writing – original draft. **Marta Romeo-Rubio:** Supervision, Visualization, Validation, Conceptualization,

Methodology, Writing – review & editing. **Jaime Del Río-Highsmith:** Supervision, Visualization, Validation, Conceptualization, Methodology, Resources, Project administration, Writing – review & editing. **Christopher D. Lynch:** Visualization, Validation, Conceptualization, Methodology, Writing – review & editing. **Raquel Castillo-Oyagüe:** Supervision, Visualization, Validation, Conceptualization, Methodology, Investigation, Project administration, Writing – original draft, Writing – review & editing.

Declaration of Competing Interest

The authors declare that they have no known competing financial interests or personal relationships that could have appeared to influence the work reported in this paper.

Acknowledgments

The authors would like to thank Dr. Tamimi, for his wise advice and for making the stay of the first author in Montreal (Canada) possible, taking part in interesting research experiences with the Craniofacial team of the McGill University. We are also grateful to Dr. Nowlan, from the Polytechnic School of the University of Montreal, for her valuable help and involvement in the bending experiment. The authors would like to express our most sincere gratitude to 'Procotech Dental Laboratory', in Madrid (Spain), for their kind cooperation, and, especially to Tony Muscia, for his personal work and expertise, who selflessly fabricated the prostheses for this study. We thank Dr. Pradíes, from the Complutense University of Madrid (UCM, Spain), for generously sharing with us the thermocycling machine and the stereo microscope of his research team. Finally, we would like to acknowledge Santiago Cano, expert in biostatistics of the Centre of Data Processing (Computing Service for Research Support of the UCM), for his assistance with the statistical analysis.

References

[1] T. Kwon, P.A. Bain, L. Levin, Systematic review of short- (5–10 years) and long-term (10 years or more) survival and success of full-arch fixed dental hybrid prostheses and supporting implants, J. Dent. 42 (2014) 1228–1241, https://doi.org/10.1016/j.jdent.2014.05.016.

[2] D. Nisand, F. Renouard, Short implant in limited bone volume, Periodontol 66 (2014) (2000) 72–96, https://doi.org/10.1111/prd.12053.

[3] M. Menéndez-Collar, M.A. Serrera-Figallo, P. Hita-Iglesias, R. Castillo-Oyagüe, J. C. Casar-Espinosa, A. Gutiérrez-Corrales, J.L. Gutiérrez-Perez, D. Torres-Lagares, Straight and tilted implants for supporting screw-retained full-arch dental prostheses in atrophic maxillae: a 2-year prospective study, Med. Oral Patol. Oral Cir. Bucal 23 (2018) e733–e741, https://doi.org/10.4317/medoral.22459.

[4] P.I. Brånemark, B. Svensson, D. van Steenberghe, Ten-year survival rates of fixed prostheses on four or six implants ad modum Branemark in full edentulism, Clin. Oral Implants Res. 6 (1995) 227–231, https://doi.org/10.1034/j.1600-0501.1995.060405.x.

[5] B. Ver gendal, S. Palmqvist, Laser-welded titanium frameworks for implant-supported fixed prostheses: a 5-year report, Int. J. Oral Maxillofac. Implants 14 (1999) 69–71.

[6] W.M. Murphy, E.G. Absi, M.C. Gregory, K.R. Williams, A prospective 5-year study of two cast framework alloys for fixed implant-supported mandibular prostheses, Int. J. Prosthodont. 15 (2002) 133–138.

[7] M. Revilla-León, L. Ceballos, I. Martínez-Klemm, M. Özcan, Discrepancy of complete-arch titanium frameworks manufactured using selective laser melting and electron beam melting additive manufacturing technologies, J. Prosthet. Dent. 120 (2018) 942–947, https://doi.org/10.1016/j.prosdent.2018.02.010.

[8] S. Taşın, I. Turp, E. Bozdağ, E. Sünbüloğlu, A. Üşümez, Evaluation of strain distribution on an edentulous mandible generated by cobalt-chromium metal alloy fixed complete dentures fabricated with different techniques: an in vitro study, J. Prosthet. Dent. 122 (2019) 47–53, https://doi.org/10.1016/j.prosdent.2018.10.034.

[9] P. Papaspyridakos, C.J. Chen, S.K. Chuang, H.P. Weber, G.O. Gallucci, A systematic review of biologic and technical complications with fixed implant rehabilitations for edentulous patients, Int. J. Oral Maxillofac. Implants 27 (2012) 102–110.

[10] B.A. Purcell, E.A. McGlumphy, J.A. Holloway, F.M. Beck, Prosthetic complications in mandibular metal-resin implant-fixed complete dental prostheses: a 5- to 9-year analysis, Int. J. Oral Maxillofac. Implants 23 (2008) 847–857.

[11] G. Priest, J. Smith, M.G. Wilson, Implant survival and prosthetic complications of mandibular metal-acrylic resin implant complete fixed dental prostheses, J. Prosthet. Dent. 111 (2014) 466–475, https://doi.org/10.1016/j.prosdent.2013.07.027.

[12] J. Ventura, E. Jiménez-Castellanos, J. Romero, F. Enrile, Tooth fractures in fixed full-arch implant-supported acrylic resin prostheses: a retrospective clinical study, Int. J. Prosthodont. 29 (2016) 161–165, https://doi.org/10.11607/ijp.4400.

[13] R.A. de Medeiros, M.C. Goiato, A.A. Pesqueira, A.J. Vechiato Filho, L. da R. Bonatto, D.M. Dos Santos, Stress Distribution in an Implant-Supported Mandibular Complete Denture Using Different Cantilever Lengths and Occlusal Coating Materials, Implant Dent 26 (2017) 106–111, https://doi.org/10.1097/ID.0000000000000534.

[14] L. Grieznis, P. Apse, L. Blumfelds, Passive tactile sensibility of teeth and osseointegrated dental implants in the maxilla, Stomatologija 12 (2010) 80–86.

[15] D.M. Davis, M.E. Packer, R.M. Watson, Maintenance requirements of implant- 203 supported fixed prostheses opposed by implant-supported fixed prostheses, natural teeth, or complete dentures: a 5-year retrospective study, Int. J. Prosthodont. 16 (2003) 521–523.

[16] Y. Zhou, J. Gao, L. Luo, Y. Wang, Does Bruxism Contribute to Dental Implant Failure? A Systematic Review and Meta-Analysis, Clin. Implant Dent. Relat. Res. 18 (2016) 410–420, https://doi.org/10.1111/cid.12300.

[17] M. Bulbul, B. Kesim, The effect of primers on shear bond strength of acrylic resins to different types of metals, J. Prosthet. Dent. 103 (2010) 303–308, https://doi.org/10.1016/S0022-3913(10)60063-7.

[18] A.J. Vechiato-Filho, I. da Silva Vieira Marques, D.M. Dos Santos, A.O. Matos, E. C. Rangel, N.C. da Cruz, et al., Effect of nonthermal plasma treatment on surface chemistry of commercially-pure titanium and shear bond strength to autopolymerizing acrylic resin, Mater. Sci. Eng. C. Mater. Biol. Appl. 60 (2016) 37–44, https://doi.org/10.1016/j.msec.2015.11.008.

[19] G. Lee, R.L. Engelmeier, M. Gonzalez, J.M. Powers, L.F. Perezous, K.L. O'Keefe, Force needed to separate acrylic resin from primed and unprimed frameworks of different designs, J. Prosthodont. 19 (2010) 14–19.

[20] R. Lang, C. Kolbeck, R. Bergmann, G. Handel, M. Rosentritt, Bond of acrylic teeth to different denture base resins after various surface-conditioning methods, Clin. Oral Investig. 16 (2012) 319–323, https://doi.org/10.1007/s00784-010-0493-8.

[21] G.E. Krueger, A.M. Diaz-Arnold, S.A. Aquilino, F.R. Scandrett, A comparison of electrolytic and chemical etch systems on the resin-to-metal tensile bond strength, J. Prosthet. Dent. 64 (1990) 610–617, https://doi.org/10.1016/0022-3913(90)90137-2.

[22] H. Strygler, J.I. Nicholls, J.D. Townsend, Microleakage at the resin-alloy interface 205 of chemically retained composite resins for cast restorations, J. Prosthet. Dent. 65 (1991) 733–739, 1016/0022-3913(90)90137-2.

[23] B. Sharp, D. Morton, A.E. Clark, Effectiveness of metal surface treatments in controlling microleakage of the acrylic resin-metal framework interface, J. Prosthet. Dent. 84 (2000) 617–622, https://doi.org/10.1067/mpr.2000.111497.

[24] S. Banerjee, R.L. Engelmeier, K.L. O'Keefe, J.M. Powers, In vitro tensile bond strength of denture repair acrylic resins to primed base metal alloys using two different processing techniques, J. Prosthodont. 18 (2009) 676–683, https://doi.org/10.1111/j.1532-849X.2009.00499.

[25] M. Menini, P. Pesce, F. Pera, F. Barberis, A. Lagazzo, L. Bertola, et al., Biological and mechanical characterization of carbon fiber frameworks for dental implant applications, Mater. Sci. Eng. C. Mater. Biol. Appl. 70 (2017) 646–655, https://doi.org/10.1016/j.msec.2016.09.047.

[26] P. Pesce, A. Lagazzo, F. Barberis, L. Repetto, F. Pera, D. Baldi, M. Menini, Mechanical characterisation of multi vs. uni-directional carbon fiber frameworks for dental implant applications, Mater. Sci. Eng. C. Mater. Biol. Appl. 102 (2019) 186–191, https://doi.org/10.1016/j.msec.2019.04.036.

[27] F. Delucchi, E. De Giovanni, P. Pesce, F. Bagnasco, F. Pera, D. Baldi, M. Menini, Framework Materials for Full-Arch Implant-Supported Rehabilitations: a Systematic Review of Clinical Studies, Materials (Basel.) 14 (2021) 3251, https://doi.org/10.3390/ma14123251.

[28] F. Pera, P. Pesce, F. Solimano, T. Tealdo, P. Pera, M. Menini, Carbon fibre versus metal framework in full-arch immediate loading rehabilitations of the maxilla - a cohort clinical study, J. Oral Rehabil. 44 (2017) 392–397, https://doi.org/10.1111/joor.12493.

[29] M. Menini, F. Pera, F. Barberis, G. Rosenberg, F. Bagnasco, P. Pesce, Evaluation of Adhesion Between Carbon Fiber Frameworks and Esthetic Veneering Materials, Int. J. Prosthodont. 31 (2018) 453–455, https://doi.org/10.11607/ijp.5786.

[30] B. Rangert, T. Jemt, L. Jörneus, Forces and moments on Branemark implants, Int. J. Oral Maxillofac. Implants 4 (1989) 241–247.

[31] R.M. Watson, D.M. Davis, G.H. Forman, T. Coward, Considerations in design and fabrication of maxillary implant-supported prostheses, Int. J. Prosthodont. 4 (1991) 232–239.

[32] E.J. Rasmussen, Alternative prosthodontic technique for tissue-integrated prostheses, J. Prosthet. Dent. 57 (1987) 198–204, https://doi.org/10.1016/0022-3913(87)90147-8.

[33] E.V. Freitas da Silva, D.M. Dos Santos, M.V. Sonego, J.M. de Luna Gomes, E. P. Pellizzer, M.C. Goiato, Does the Presence of a Cantilever Influence the Survival and Success of Partial Implant-Supported Dental Prostheses? Systematic Review and Meta-Analysis, Int. J. Oral Maxillofac. Implants 33 (2018) 815–823, https://doi.org/10.11607/jomi.6413.

[34] V.F. Ferrario, C. Sforza, G. Zanotti, G.M. Tartaglia, Maximal bite forces in healthy young adults as predicted by surface electromyography, J. Dent. 32 (2004) 451–457, https://doi.org/10.1016/j.jdent.2004.02.009.

[35] C.C. Serdar, M. Cihan, D. Yücel, M.A. Serdar, Sample size, power and effect size revisited: simplified and practical approaches in pre-clinical, clinical and laboratory studies, Biochem. Med. (Zagreb). 31 (2021), 010502, https://doi.org/10.11613/BM.2021.010502.

[36] R.C. Oyagüe, M.I. Sánchez-Jorge, A. Sánchez Turrión, Evaluation of fit of zirconia posterior bridge structures constructed with different scanning methods and preparation angles, Odontology 98 (2010) 170–172, https://doi.org/10.1007/s10266-010-0122-7.
[37] K. Nakazawa, K. Nakamura, A. Harada, M. Shirato, R. Inagaki, U. Örtengren, T. Kanno, Y. Niwano, H. Egusa, Surface properties of dental zirconia ceramics affected by ultrasonic scaling and low-temperature degradation, PLoS ONE 13 (2018), e0203849, https://doi.org/10.1371/journal.pone.0203849.
[38] E.T. Giampaolo, J.H. Jorge, A.L. Machado, A.C. Pavarina, C.E. Vergani, Effect of thermal cycling on microleakage between hard chairside relines and denture base acrylic resins, Gerodontology 28 (2011) 121–126, https://doi.org/10.1111/j.1741-2358.2009.00332.x.
[39] R. Castillo-de-Oyagüe, A. Sánchez-Turrión, J.F. López-Lozano, A. Albaladejo, D. Torres-Lagares, J. Montero, et al., Vertical misfit of laser-sintered and vacuum-cast implant-supported crown copings luted with definitive and temporary luting agents, Med. Oral Patol. Oral Cir. Bucal 17 (2012) e610–e617, https://doi.org/10.4317/medoral.17997.
[40] R. Castillo Oyagüe, M.I. Sánchez-Jorge, A. Sánchez Turrión, Influence of CAD/CAM scanning method and tooth-preparation design on the vertical misfit of zirconia crown copings, Am. J. Dent. 23 (2010) 341–346. PMID: 21344834.
[41] S.S. Shapiro, M.B. Wilk, An analysis of variance test for normality (complete samples), Biometrika 52 (1965) 591–611, https://doi.org/10.1093/biomet/52.3-4.591.
[42] J. Goldberg, G. Ronaghi, J.H. Phark, S. Jivraj, W. Chee, Force-to-failure of a simulated implant-supported complete fixed dental prosthesis reinforced with glassfiber, J. Prosthet. Dent. 118 (2017) 172–176, https://doi.org/10.1016/j.prosdent.2016.11.010.
[43] R. Castillo-de Oyagüe, C. Lynch, R. McConnell, N. Wilson, Teaching the placement of posterior resin-based composite restorations in Spanish dental schools, Med. Oral Patol. Oral Cir. Bucal 17 (2012) e661–e668, https://doi.org/10.4317/medoral.17656.
[44] C.E. Misch, Contemporary Implant Dentistry, Mosby Elsevier, St. Louis (MO), 2007 third ed.
[45] F. Egilmez, G. Ergun, I. Cekic-Nagas, S. Bozkaya, Implant-supported hybrid prosthesis: conventional treatment method for borderline cases, Eur. J. Dent. 9 (2015) 442–448, https://doi.org/10.4103/1305-7456.163324.
[46] L.T. Yong, P.K. Moy, Complications of computer-aided-design/computer-aided-machining-guided (NobelGuide) surgical implant placement: an evaluation of early clinical results, Clin. Implant Dent. Relat. Res. 10 (2008) 123–127, https://doi.org/10.1111/j.1708-8208.2007.00082.x.
[47] I.E. Ruyter, K. Ekstrand, N. Bjork, Development of carbon/graphite fiber reinforced poly (methyl methacrylate) suitable for implant-fixed dental bridges, Dent. Mater. 2 (1986) 6–9, https://doi.org/10.1016/s0109-5641(86)80062-8.
[48] N. Björk, K. Ekstrand, I.E. Ruyter, Implant-fixed, dental bridges from carbon/graphite ibre reinforced poly(methyl methacrylate), Biomaterials 7 (1986) 73–75, https://doi.org/10.1016/0142-9612(86)90093-1.
[49] S. Segerström, G. Sandborgh-Englund, E.I. Ruyter, Biological and physicochemical properties of carbon-graphite fibre-reinforced polymers intended for implant suprastructures, Eur. J. Oral Sci. 119 (2011) 246–252, https://doi.org/10.1111/j.1600-0722.2011.00826.x.
[50] S. Segerström, I.E. Ruyter, Adhesion properties in systems of laminated pigmented polymers, carbon-graphite fiber composite framework and titanium surfaces in implant suprastructures, Dent. Mater. 25 (2009) 1169–1177, https://doi.org/10.1016/j.dental.2009.04.009.
[51] S. Segerström, I.E. Ruyter, Mechanical and physical properties of carbon-graphite fiber-reinforced polymers intended for implant suprastructures, Dent. Mater. 23 (2007) 1150–1156, https://doi.org/10.1016/j.dental.2006.06.050.
[52] T. Bergendal, K. Ekstrand, U. Karlsson, Evaluation of implant-supported carbon/graphite fiber-reinforced poly (methyl methacrylate) prostheses. A longitudinal multicenter study, Clin. Oral Implants Res. 6 (1995) 246–253, https://doi.org/10.1034/j.1600-0501.1995.060408.x.
[53] J. Tinschert, D. Zwez, R. Marx, K.J. Anusavice, Structural reliability of aluminafeldspar-leucite-, mica- and zirconia-based ceramics, J. Dent. 28 (2000) 529–535, https://doi.org/10.1016/s0300-5712(00)00030-0.
[54] J. Schmitt, S. Holst, M. Wichmann, S. Reich, M. Gollner, J. Hamel, Zirconia posterior fixed partial dentures: a prospective clinical 3-year follow-up, Int. J. Prosthodont. 22 (2009) 597–603.
[55] C. López-Suárez, R. Castillo-Oyagüe, V. Rodríguez-Alonso, C.D. Lynch, M.J. Suárez-García, Fracture load of metal-ceramic, monolithic, and bi-layered zirconia-based posterior fixed dental prostheses after thermo-mechanical cycling, J. Dent. 73 (2018) 97–104, https://doi.org/10.1016/j.jdent.2018.04.012.
[56] J.A. Ribeiro, C.M. de Resende, A.L. Lopes, W. Mestriner Jr., A.G. Roncalli, A. Farias-Neto, F. Carreiro, F. Ada, Evaluation of complete denture quality and masticatory efficiency in denture wearers, Int. J. Prosthodont. 25 (2012) 625–630.
[57] E. Jasser, Z. Salami, F. El Hage, J. Makzoumé, P.J. Boulos, Masticatory Efficiency in Implant-Supported Fixed Complete Dentures Compared with Conventional Dentures: a Randomized Clinical Trial by Color-Mixing Analysis Test, Int. J. Oral Maxillofac. Implants 35 (2020) 599–606, https://doi.org/10.11607/jomi.7911.
[58] T. Pereira-Cenci, L.J. Pereira, M.S. Cenci, W.C. Bonachela, A.A. Del Bel Cury, Maximal bite force and its association with temporomandibular disorders, Braz. Dent. J. 18 (2007) 65–68, https://doi.org/10.1590/s0103-64402007000100014.
[59] K. Masouras, N. Silikas, D.C. Watts, Correlation of filler content and elastic properties of resin-composites, Dent. Mater. 24 (2008) 932–939, https://doi.org/10.1016/j.dental.2007.11.007.
[60] N.M. Ajaj-Alkordy, M.H. Alsaadi, Elastic modulus and flexural strength comparisons of high-impact and traditional denture base acrylic resins, Saudi Dent. J. 26 (2014) 15–18, https://doi.org/10.1016/j.sdentj.2013.12.005.
[62] L. Hassouneh, A.A. Jum'ah, M. Ferrari, D.J. Wood, Post-fatigue fracture resistance of premolar teeth restored with endocrowns: an in vitro investigation, J. Dent. 100 (2020), 103426, https://doi.org/10.1016/j.jdent.2020.103426.
[61] A. Preciado, J. Del Río, C.D. Lynch, R. Castillo-Oyagüe, A new, short, specific questionnaire (QoLIP-10) for evaluating the oral health-related quality of life of implant-retained overdenture and hybrid prosthesis wearers, J. Dent. 41 (2013) 753–763, https://doi.org/10.1016/j.jdent.2013.06.014.
[63] R. Castillo-Oyagüe, M.J. Suárez-García, C. Perea, J.D. Río, C.D. Lynch, E. Gonzalo, et al., Validation of a new, specific, complete, and short OHRQoL scale (QoLFAST-10) for wearers of implant overdentures and fixed- detachable hybrid prostheses, J. Dent. 49 (2016) 22–32, https://doi.org/10.1016/j.jdent.2016.04.011.